Three-dimensional Fatigue Crack Evaluation Using Densely Connected Convolutional Network-assisted Nonlinear Ultrasonics

Lei Xu [a,b*], Jianwei Yang [a,b], Ming Ge [a,c] and Zhongqing Su [b]

[a] Robotics and Artificial Intelligence Division, Hong Kong Productivity Council, Kowloon, Hong Kong SAR

[b] Department of Mechanical Engineering, The Hong Kong Polytechnic University, Kowloon, Hong Kong SAR

[c] Hong Kong Industrial Artificial Intelligence and Robotics Centre (FLAIR), Shatin, New Territories, Hong Kong SAR

submitted to ***International Journal of Fatigue***

(submitted on XXX 2023)

Abstract

Linear and nonlinear ultrasonic guided wave (UGW)-based methods are available for detection and evaluation of fatigue cracks and monitor the growth under cyclic loadings. However, linear methods usually fail to detect early-stage fatigue cracks of undersized dimensions, while nonlinear methods struggle to assess cracks once they have extended to a certain degree. The fusion of linear and nonlinear UGW features offers new opportunity to enhance evaluation precision and effectiveness, yet it necessitates highly complex theoretical modeling. Motivated by this, densely connected convolutional network-based regression model using the spectra of UGW signals is proposed in this study for the evaluation of three-dimensional (3D) fatigue cracks from embryonic initiation, through progressive growth to the formation of macroscopic cracks. Via the continuous wavelet transform (CWT), the spectra of UGW signals captured during fatigue crack initiation and growth are obtained, which embrace both linear and nonlinear features of UGW. Subsequently, spectra images are used as the input of the famed densely connected convolutional network, DenseNet, to extract the implicit features of UGW. Finally, the last fully connected layer of the DenseNet is modified as a regression layer to predict the length and depth of 3D fatigue cracks. For validating the proposed model, a dataset with a total number of 400 UGW signals is established based on the experiment and simulation of 3D corner crack growth. A comparison study is conducted between the proposed DenseNet-based regression model and a previously reported nonlinear UGW-based model for 3D corner crack evaluation. Results show that the proposed model can characterize the length and depth of a corner crack in both initiation and growth stages. The proposed model represents a promising proof-of-concept for deep learning-based quantitative evaluation of 3D fatigue cracks.

***Keywords*:** Deep learning-based regression; densely connected convolutional network; ultrasonic guided wave; 3D fatigue crack, quantitative evaluation

1. Introduction

Fatigue cracks are widely found in critical components of engineering structures, which are liable for numerous sudden catastrophic failures of entire structures, such as flight vehicles, rail tracks, infrastructures, and so on. It is reported that fatigue is associated with over 90 % of all mechanical failures [1]. Therefore, early awareness, continuous monitoring, and accurate evaluation of fatigue cracks are of great significance for ensuring the integrity and safety of structures. For this purpose, ultrasonic guided wave (UGW)-based methods have been developed to detect and characterize both macroscopic and small-scale fatigue cracks [2-7]. The principle of UGW-based fatigue crack identification and assessment rests on the idea that the propagation characteristics of a probing UGW undergo a certain degree of modulation and alteration upon interaction with a fatigue crack. This UGW-crack interaction gives rise to distinct wave scattering phenomena, including reflection, transmission, mode conversion, resonant frequency shift, wave energy transfer, and the generation of higher- and sub-order harmonics. Therefore, fatigue cracks can be inversely identified and evaluated through careful examination of the alterations in UGW attributes by employing suitable analytical models.

Linear UGW-based methods making use of linear wave features such as the reflection and transmission coefficients [8-11], delay in time-of-flight [12], degree of wave energy dissipation [13], and mode conversion [14], have been widely applied to identify fatigue cracks. These linear methods show particular effectiveness in detecting and evaluating fatigue cracks with the characteristic dimensions comparable to the wavelength of the probing UGW - a scale at which the cracks may have already progressed to a macroscopic extent, resulting in a magnitude substantial enough to induce fatal structural failure. To detect the small-scale fatigue cracks as early as possible, nonlinear UGW-based methods have been proposed recently, making up for the shortcomings of linear methods in identifying imperceptible fatigue cracks. Approaches in this category can be broadly classified into harmonic generation [2, 15-18], resonant frequency shift

[19] and wave mixing [20-22]. Representatively, Xiang *et. al.* [23] developed a model to correlate the fatigue crack location with the wavelet coefficients at the second harmonic frequency of Lamb waves, which can be applied for the localization of barely visible fatigue cracks. Based on the elastodynamic reciprocity theorem, Xu *et. al.* [24] proposed an analytical model to shed light on the second harmonic generation arise from the contact acoustic nonlinearity (CAN) at 'breathing' cracks and derived a closed-form solution to the magnitude of crack-induced second harmonic, which can be employed for detection and characterization of tiny fatigue cracks. Shen *et. al.* [25] proposed a nonlinear ultrasonic resonance spectral correlation technique for fatigue crack quantification and tailored a nonlinear reduced-order oscillator model to illuminate the CAN at the fatigue cracks. Results demonstrated that the proposed technique is able to detect fatigue cracks as short as 1.5 mm. Sohn *et. al.* [4, 26] designed the two-wave and three-wave mixing techniques in which two or three UGWs with distinct central frequencies are excited in the targeted structure simultaneously and the nonlinear sideband harmonics will appear at the sum and difference of the input frequencies due to the existence of fatigue cracks. The crack-induced sideband harmonics are inversely used to detect and localize early-stage fatigue cracks and provide timely warning of imminent failure.

Although the use of linear features of UGW proves particularly efficient when the characteristic dimensions of targeted fatigue cracks are comparable to the wavelength of the probing UGW and the nonlinear UGW is adept at detecting incipient fatigue cracks, both methodologies fall short in providing reliable identification and assessment of fatigue cracks throughout their early-stage initiation and stable growth phases. The fusion of linear and nonlinear attributes of UGW presents a viable solution to overcome this limitation, yet intricate modeling is imperative to establish a correlation between these wave attributes and fatigue crack severity, due to the diverse UGW-crack interaction mechanisms that vary across different stages of crack evolution. Amongst limited effort, Kundu *et. al.* [27] proposed a holistic technique for sensing impact damage

initiation and progression in composite plates, by combining linear and nonlinear features of UGW. In that technique, the evolution of impact damage is divided into early, intermediate, and advanced stages. The linear and nonlinear UGW were applied to evaluate damage in the early and advanced stages, respectively, and the joint use of both shown effectiveness in the intermediate stage. There is an absence of foundational analysis correlating linear and nonlinear damage indicators with damage severity, as well as the precise demarcation of the three stages of damage evolution. Consequently, this shortfall poses challenges in practical applications of the holistic technique for damage evaluation.

Recent years have witnessed the rapid development of deep learning (DL) and its successful applications in various fields such as image recognition, natural language processing, speech recognition, and no exception for crack detection in engineering structures. To deal with the detection of cracks in concrete bridges, Deng *et. al.* [28] applied the You Only Look Once (YOLO) model to automatically locate the concrete cracks with bounding box from raw real-world images contaminated with handwriting scripts. Long *et. al.* [29] proposed a novel global and local dual-scale faster region-based convolutional neural network (Faster R-CNN) to predict the fatigue crack length based on the images captured by a camera. Results demonstrate that the proposed method can effectively measure the propagating small cracks during cyclic loading and can be applied for fatigue crack growth rate measurement. Based on the UGW method, Sohn *et. al.* [30] designed a hybrid framework that incorporates higher-order spectral analysis of Lamb waves with a long short-term memory (LSTM)-based DL model for early detection of fatigue cracks. Results validated the robustness of the proposed framework for reliable fatigue crack detection in noisy environments. Guo *et. al.* [31] used three pre-trained DL models (*e.g.*, VGG16, ResNet50, and DenseNet161) to extract features from laser-generated ultrasonic waves and developed a multiplicative LSTM (mLSTM)-based classifier for automatic quantification of subsurface defects. Defects with the dimensions ranging from 0.2 mm to 6.0 mm were divided

into 30 categories and the trained mLSTM-based classifier can predict the defect size with an overall accuracy of 98.26 %.

Previous studies have shown that DL possesses the advantage of establishing implicit connections between physical quantities. This superb merit enables it to circumvent the intricate mathematical modeling necessitated by the fusion of linear and nonlinear features of UGW for fatigue crack evaluation from small-scale initiation to macroscopic evolution. On the other hand, although good supply of research has been conducted based on DL-based classification for fatigue crack detection and assessment, there are very few regression models for the continuous monitoring and evaluation of embryonic three-dimensional (3D) fatigue cracks which do not penetrate the entire thickness of the structures. Different from the two-dimensional (2D) fatigue cracks penetrating the entire thickness of structures which have been investigated extensively, 3D, non-penetrating cracks grow in both length and depth directions under cyclic loading, as schematically illustrated in **Fig. 1**. 3D fatigue cracks, represented by surface cracks and corner cracks, play a vital role in damage tolerance assessment and health monitoring of engineering structures, as the fatigue life in the 3D, non-penetrating stage accounts for more than 80 % of the total fatigue life [32-34]. Therefore, it is of great significance to develop a regression model to continuously monitor and accurately evaluate the 3D fatigue cracks from their initiation to the macroscopic progression.

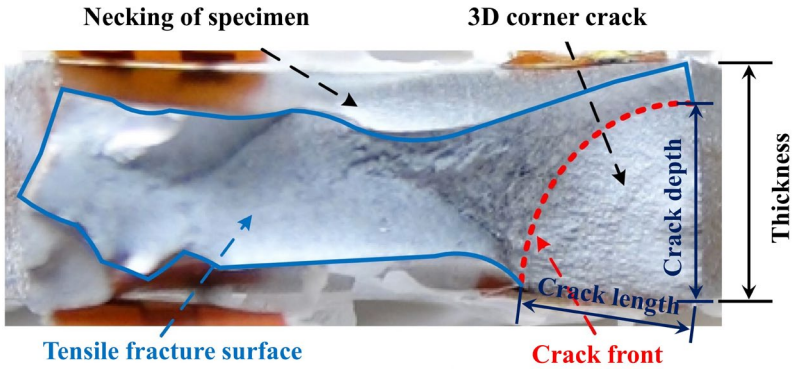

Fig. 1. Schematic of a representative 3D corner crack and its progressive evolution under fatigue loading [35].

In recognition of the lack of DL-based regression able to monitor the growth and evaluate the severity (*i.e.*, crack length and depth) of 3D fatigue cracks, a regression model based on the famed densely connected convolutional network, DenseNet [36], is proposed in this study, using the spectra of UGW which embrace both linear and nonlinear wave features. By performing a time-frequency analysis via the continuous wavelet transform (CWT), the spectra of raw UGW signals measured during the initiation and growth stages of a 3D fatigue crack are obtained. The DenseNet is subsequently recalled for extracting time-frequency domain implicit features from the UGW spectra images. The last fully connected layer of DenseNet is further modified as a regression layer to predict the length and depth of the 3D fatigue crack. Both experiment and simulation are performed to acquire the UGW signals during the initiation and growth stages of a 3D corner crack emanating from a fastener hole, the most widely detected 3D fatigue crack in engineering structures. Real-world and simulated UGW signals are collected to establish a dataset for the training and validation of the proposed model. A comparison study between the proposed DenseNet-based regression model and the previously reported model combining nonlinear UGW and fatigue crack growth theory is conducted. Results demonstrate that the proposed model is not only able to evaluate the corner cracks in the initiation and early progressive growth stage, but can also predict the crack length and depth accurately when a macroscopic fatigue crack is formed. This provides a new way for life-cycle monitoring and assessment of fatigue cracks.

2. DenseNet-based Regression for 3D Fatigue Crack Evaluation

The framework of the proposed DenseNet-based regression model for 3D fatigue crack evaluation is detailed in this section. Firstly, the CWT is adopted to obtain the spectra of raw UGW signals in the time-frequency domain. Subsequently, the spectra images are used as the input to train the DenseNet with the last fully connected layer being modified to a regression layer for predicting the length and depth of 3D fatigue cracks.

2.1 Time-frequency Feature Extraction Via CWT

The CWT stands as a pivotal mathematical technique extensively employed in signal processing and analysis. Derived from the broader framework of the wavelet transform, the CWT offers a means to scrutinize the time-frequency representation of a signal in a continuous manner, making it particularly adept at capturing localized features in the time-frequency domain. Different from the discrete wavelet transform (DWT) which dissects a signal into discrete segments of varying scale, the CWT permits an adaptable window function that can be dynamically adjusted to capture intricate signal components across various scales. This flexibility in window size facilitates a nuanced exploration of signal characteristics, which is essential in applications spanning diverse fields such as image processing, audio analysis, and biomedical signal interpretation.

In the proposed model, the CWT is adopted to extract the time-frequency domain features and obtain the spectra of raw UGW signals captured throughout the fatigue crack initiation and growth stages. For a given raw UGW signal $s(t)$, the CWT is performed via the following integral manipulation, as

$$S_{\omega}(a,b)=\frac{1}{|a|^{1/2}}\int_{-\infty}^{\infty}s(t)\overline{\psi}(\frac{t-b}{a})dt, \tag{1}$$

where $a\in R^{+}$ is the scale indicator and $b\in R^{+}$ is the translational value. The overline represents the operation of complex conjugate and $\psi(\cdot)$ represents the mother wavelet which is a continuous function in both time and frequency domains. In the proposed model, the morse wavelet is utilized as the mother wavelet to acquire the spectra of measured UGW signals.

2.2 DenseNet-based Regression for 3D Crack Evaluation

After obtaining the spectra of raw UGW signals via the CWT, a DL-based regression model is employed to extract implicit features from the spectra images for the prediction of the length and depth of 3D fatigue cracks. The DenseNet, a highly sophisticated densely connected convolutional

network with a number of compelling merits over other powerful convolutional neural network (CNN) models such as VGG and ResNet, is utilized for the feature extraction and 3D fatigue crack evaluation. The DenseNet comprises interconnected dense blocks which are chained sequentially, interspersed with transition layers placed between contiguous dense blocks. Each dense block is composed of multiple densely connected convolutional layers. The architecture of the DenseNet and the details of a dense block are shown in **Fig. 2**.

The core principle underpinning the DenseNet is the dense connectivity pattern it introduces among layers within a dense block. In contrast to traditional CNN architectures (*i.e.*, VGG and ResNet) where information flows in a linear sequential manner, DenseNet establishes dense interconnections between layers, enabling each layer to receive input not only from its very first preceding layer but also from all preceding layers. This distinctive structural attribute engenders a rich feature propagation mechanism, efficaciously promoting information exchange and reusability throughout the entire network. By fostering these dense connections, DenseNet combats the vanishing gradient issue, which exceedingly hampers the training of deep networks. Additionally, the architecture's compactness and parameter efficiency render it conducive to learning features from relatively small datasets. Therefore, the DenseNet is an appropriate model to perform feature extraction and learning for 3D fatigue crack evaluation, considering the difficulties in constructing a big dataset consisting of thousands of UGW signals.

With the manipulation of the dense blocks and transition layers, the implicit features carried by the spectra of the raw UGW signals are extracted. Ultimately, the last fully connected layer of the DenseNet is modified as a regression layer with two outputs, for the prediction of the two characteristic indicators of 3D fatigue cracks, *i.e.*, crack length and depth. **Fig. 2** recaps the overall framework of the proposed DenseNet-based regression model.

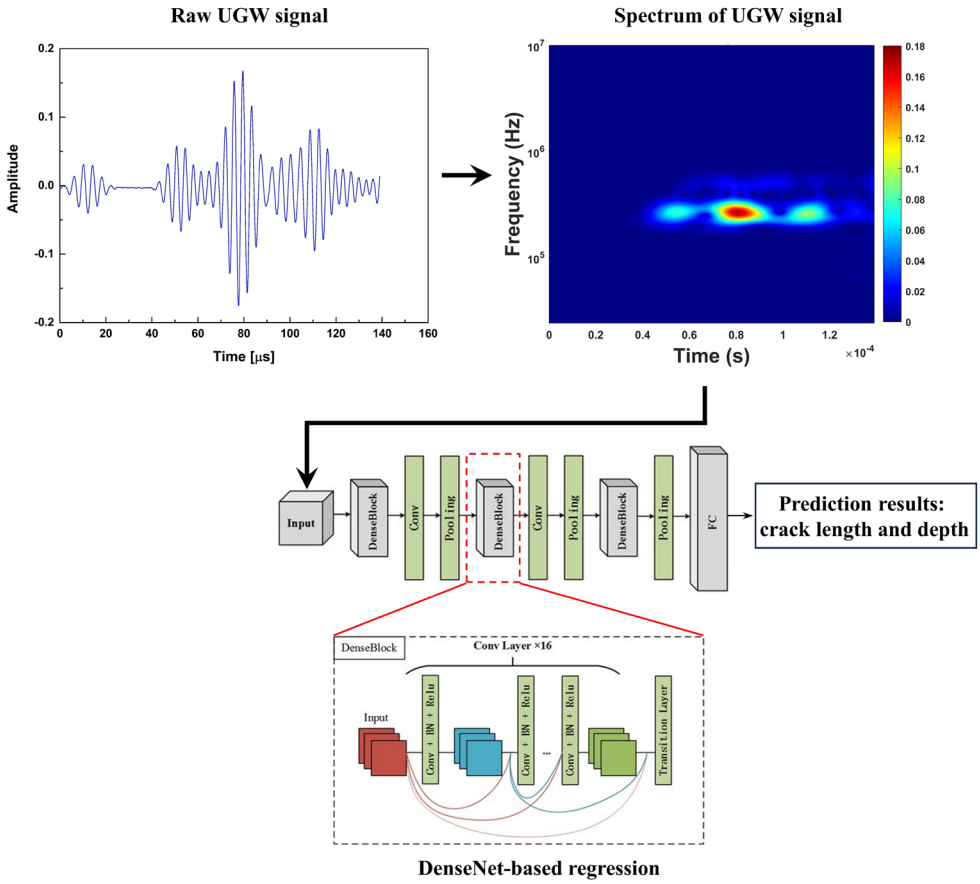

Fig. 2. Framework of the proposed DenseNet-based regression model for 3D fatigue crack evaluation.

3. Experiment and Simulation for Data Generation

For constructing a dataset for the training and validation of the proposed DenseNet-based regression model, fatigue crack growth and ultrasonic testing is performed, in which UGW signals are collected throughout the initiation and growth stages of 3D corner cracks emanating from a fastener hole. Considering the dataset based on pure experimental data is relatively small for the training of a DL model, numerical simulation is further conducted using the finite element method (FEM) to obtain synthetic UGW signals for dataset expansion.

3.1 Data Generation based on Fatigue Crack Growth and Ultrasonic Testing

Two aluminum plate-like specimens (labeled as Specimen 1 and Specimen 2, respectively), measuring 500 mm in length, 80 mm in width, and 3 mm in thickness, are prepared for the fatigue

crack growth testing. A through-thickness fastener hole with a diameter of 6 mm is drilled in the center of each specimen and a triangular artificial notch is inscribed at the fastener hole in the plane perpendicular to the direction of fatigue loading, so that a corner crack can initiate and progress under the cyclic loading. Three lead zirconate titanate (PZT) wafers are mounted on the surface of the specimen, one acting as the actuator to excite probing UGW and the other two severing as the UGW sensors to capture propagating UGW signals, as shown in **Fig. 3**. The actuator is 100 mm from the center of the fastener hole and the two sensors are placed on the other side of the hole with the distance of 100 mm and 150 mm from the hole center, respectively.

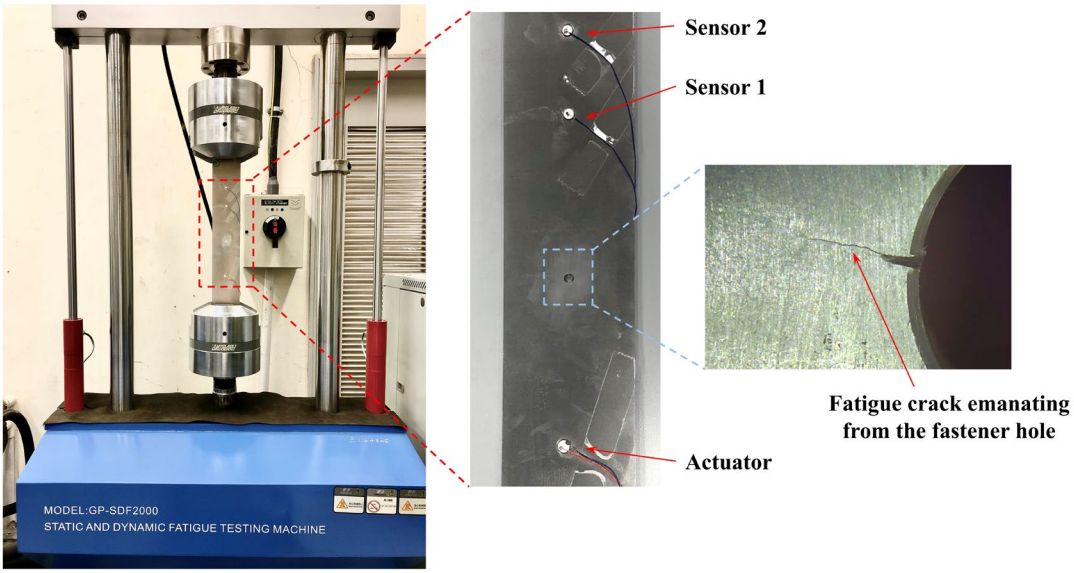

Fig. 3. Set-up of the fatigue crack growth testing and the tested specimen with a 3D corner crack emanating from the fastener hole.

A fatigue testing machine (model: GP-SDF2000) is utilized to perform the fatigue crack growth testing. A pre-cracking fatigue loading with the maximum tensile load of 30 kN and the stress ratio of 0.1 is first applied to introduce an embryonic 3D corner crack from the tip of the artificial notch at the fastener hole. The length (dimension in the specimen surface) and depth (dimension in the thickness direction of specimen) of the corner crack are continuously monitored by a microscope and a slender mirror inserted into the fastener hole. Once the embryonic corner crack

grows to an extent of ~ 1 mm in length and depth, the pre-cracking stage is suspended and the fatigue loading is regulated to 2~20 kN with a frequency of 10 Hz, to perform the growth testing of the 3D corner crack. The PZT wafers are mounted onto the specimen after the pre-cracking stage to minimize the risk of debonding between wafers and specimen. The fatigue crack growth testing is paused every 1,000 cycles, to measure the length and depth of the corner crack and conduct ultrasonic testing to acquire UGW signals. The test is terminated when the 3D corner crack penetrates the specimen thickness and a 2D, through-thickness crack is formed.

During each pause of the fatigue crack growth testing, ultrasonic testing is performed to obtain crack-modulated UGW signals. A high-power ultrasonic measurement system (RITEC® RAM-5000 SNAP) is used to excite the actuator to generate a 5-cycle Hanning-windowed sinusoidal toneburst at a central frequency of 250 kHz into the specimen. Upon modulated by the corner crack, the propagating UGW is captured by the two sensors with an oscilloscope at a sampling frequency of 200 MHz. The UGW signals are averaged 1,024 times to reduce the measurement uncertainty from testing system and environment. **Fig. 4** schematically displays the set-up of the ultrasonic testing.

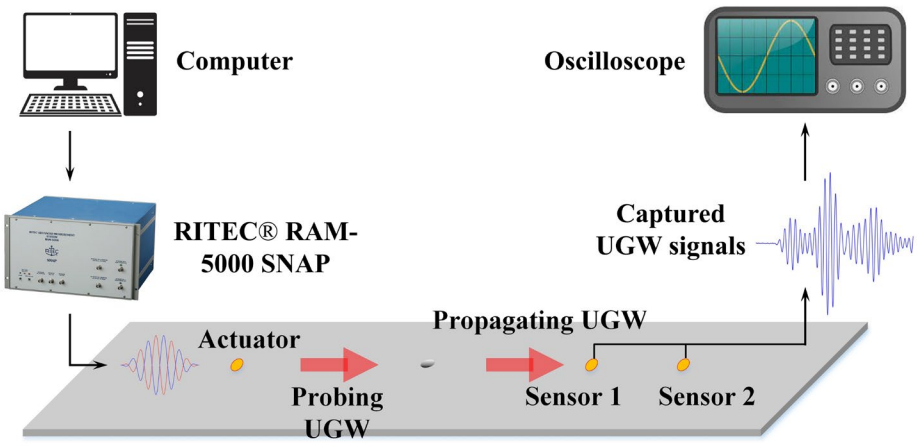

Fig. 4. Schematic of the ultrasonic testing set-up for acquiring UGW signal data during the fatigue crack initiation and growth stages.

To acquire more UGW signals in the ultrasonic testing during the pause of fatigue testing, a pulse-inversion technique [37], in which two identical probing UGWs with the same magnitude but in opposite phase are excited, is adopted in the experiment. With this technique, 4 UGW signals can be obtained by the two sensors in a single pause. The UGW signal data acquired from the entire fatigue crack growth testing of Specimen 1 and Specimen 2 are collected to construct a dataset for the training and validation of the proposed model.

3.2 Dataset Expansion with FEM Simulation

A sufficiently large dataset is of the utmost importance for training a DL model and enabling it to learn and infer from new data, while the dataset constructed based on the UGW signals acquired from the experiment in Section 3.1 is relatively small. Consequently, FEM simulation is conducted using the commercial software ABAQUS®/EXPLICIT to generate synthetic UGW signals for dataset expansion. A plate-like waveguide finite element (FE) model (density: 2700 kg/m3; Young's modulus: 73 GPa; Poisson's ratio: 0.33) with the same geometrical configuration as the tested specimens is built, as shown in **Fig. 5**. A series of semi-elliptical corner cracks with various severities (crack length and depth ranging from 1 to 3 mm) are simulated at the fastener hole and in each simulated case, the crack surface is perpendicular to the length direction of the waveguide. Material nonlinearity is not considered in the simulation due to its negligible intensity compared with the CAN induced by fatigue cracks, according to the results of previous studies [38, 39]. No special boundary layers (*e.g.*, perfect matching layer (PML) or absorbing layer with increased damping (ALID)) are set around the waveguide model to simulate the actual boundary reflection of probing UGW and to make the synthetic signals more approximate to real-world UGW signals.

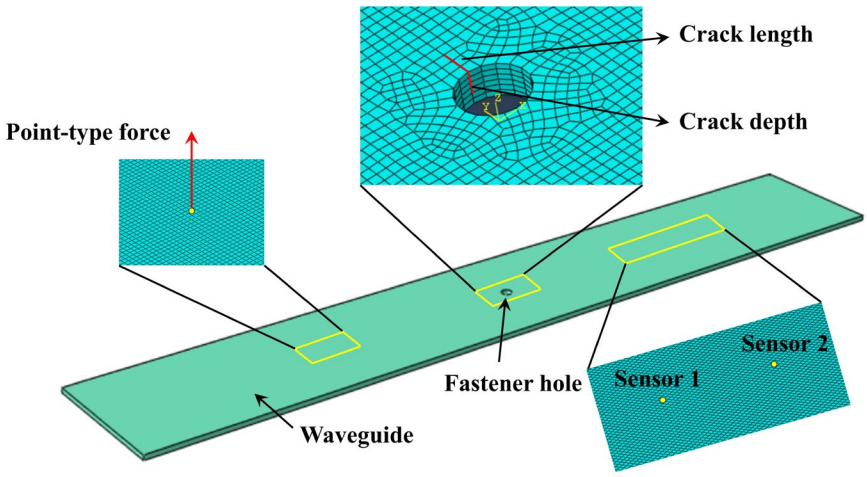

Fig. 5. FE model of the waveguide containing a semi-elliptical corner crack emanating from a fastener hole.

To generate a probing UGW in the waveguide, a toneburst with the same cycle and frequency as the excitation signal used in the experiment is excited by applying a point-type force at a node on the surface of the waveguide, as illustrated in **Fig. 5**. Two other nodes are further selected as the sensing points to capture propagating UGW signals. The locations of the excitation and sensing points are referred to the installation placement of the three PZT wafers in the experiment. Synthetic UGW signals obtained from the FEM simulation are added into the dataset consisting of experimental signals for dataset expansion for the training and validation of the proposed DenseNet-based regression model.

4. Results and Discussion

To validate the developed DenseNet-based regression model, the experimental and simulated UGW signals are converted to RGB images via the CWT, by which means an image dataset is built for training and verifying the proposed model. A comparison study is further conducted between the proposed model and a previously reported nonlinear UGW-based model, to reveal the superiority of the proposed DenseNet-based regression model in evaluating 3D fatigue cracks in both embryonic initiation and progressive growth stages.

4.1 Experimental Results and Verification of FEM Simulation

The length and depth of the corner crack emanating from the fastener hole in Specimen 1 and Specimen 2 are measured by the microscope continuously at every pause of the fatigue crack growth testing, as shown in **Fig. 6**. It can be observed that under the cyclic fatigue loading, the 3D corner crack initiates in the first a few kilocycles, then progressively grows in both length and depth directions, and eventually penetrates the entire thickness of the specimen and forms a 2D crack. By way of illustration using Specimen 1, the corner crack initiates before 9, 000 fatigue cycles and the length and depth of the corner crack remain largely unchanged during this period. After 8, 000 cycles, the crack length and depth increase with respect to fatigue cycles. The crack depth reaches 3 mm at 18, 000 cycles, indicating that the corner crack penetrates the whole thickness of the specimen and the fatigue crack growth testing is terminated accordingly. Typical photographs of the corner crack in different stages are displayed in **Fig. 7**, showing the evolution of the corner crack in both length and depth directions under the cyclic loading.

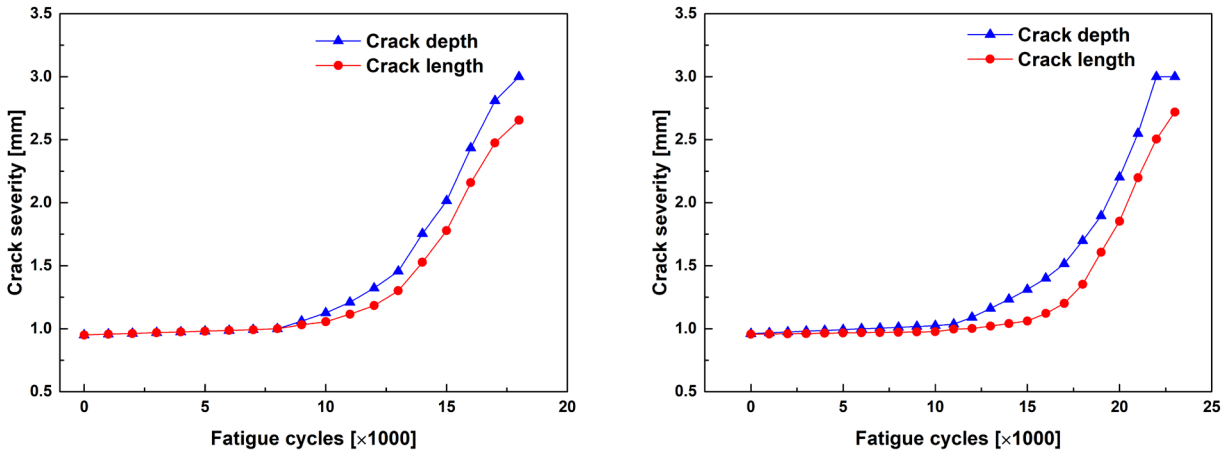

(a) (b)

Fig. 6. Measured length and depth of the corner crack emanating from the fastener hole in (a) Specimen 1; and (b) Specimen 2.

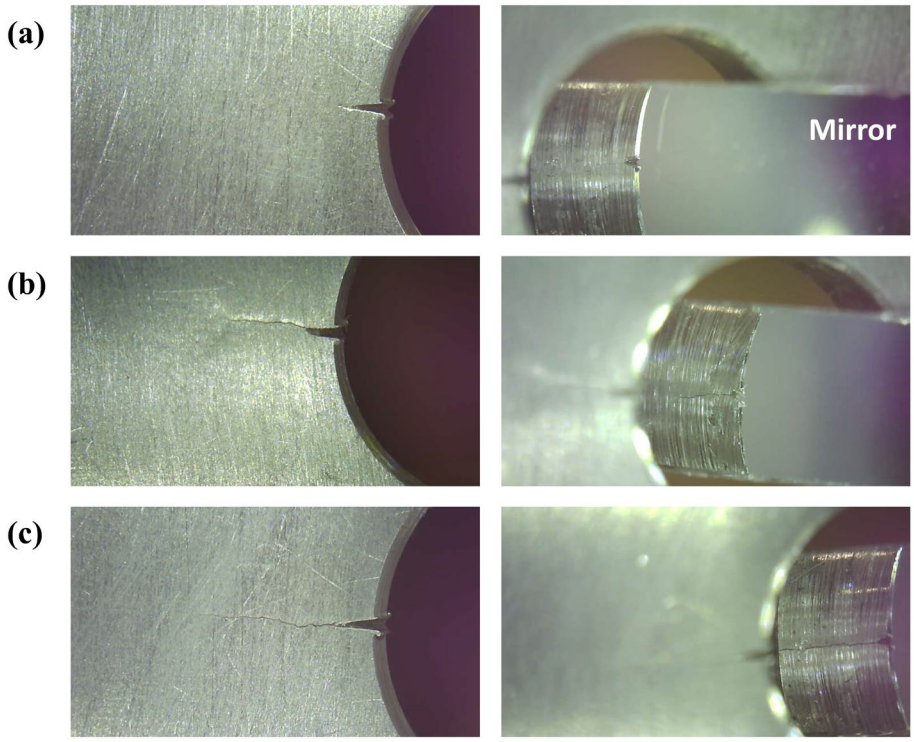

Fig. 7. Photographs of the corner crack in Specimen 1 in (a) crack initiation stage; (b) progressive growth stage; and (c) when the corner crack penetrates the whole thickness of the specimen. Left column: crack length, right column: crack depth.

As depicted in **Fig. 6,** the fatigue testing for Specimen 1 is terminated at 18,000 cycles when the corner crack penetrates the whole thickness of the specimen, while for Specimen 2, it concludes at 23,000 cycles. The fatigue testing for the two specimens is paused every 1,000 cycles for conducting ultrasonic testing to acquire UGW signals, indicating that the fatigue testing of the two specimens is paused 19 and 24 times (ultrasonic testing is also performed at 0 cycle) for ultrasonic measurement, respectively. By taking advantage of the pulse-inversion technique, 4 UGW signals can be obtained by the two sensors mounted on the specimen in a single pause, resulting in a total of 172 UGW signals acquired in the experiment.

Representative UGW signals captured by Sensor 1 mounted on Specimen 1 at different fatigue cycles are shown in **Fig. 8 (a)**. It can be observed from the raw signals that the magnitude of the signals, a typical linear feature of UGW, varies against the fatigue cycles, while the phase and

363 waveform remain largely unchanged. By performing CWT, the time-domain UGW signals
364 displayed in **Fig. 8 (a)** are converted to RGB images representing the time-frequency spectra of
365 the original signals, as shown in **Fig. 8 (b)**. A rectangular window function is utilized before the
366 implementation of the CWT, to eliminate the effect of the crosstalk interference in the raw signals
367 induced by the measurement instruments. It can be found that during the crack initiation period
368 (*i.e.*, 0 cycle and 9,000 cycles), the spectra of UGW signals only contain linear components at the
369 fundamental frequency (250 kHz). On the contrary, apart from linear components, nonlinear
370 components at higher frequency range can be found in the spectra of UGW signals captured during
371 the crack growth stage (*i.e.*, 13,000 cycles and 17,000 cycles). This can be attributed to the CAN
372 induced by the 'breathing' behavior of fatigue cracks, which has been extensively scrutinized in
373 previous studies [3, 40-42]. The personified 'breathing' describes the periodic opening and closing
374 of a fatigue crack during the propagation of a probing UGW, causing the nonlinear modulation of
375 the crack on the probing UGW and the resultant higher-order harmonic generation which can be
376 clearly seen in **Fig. 8 (b)**.
377

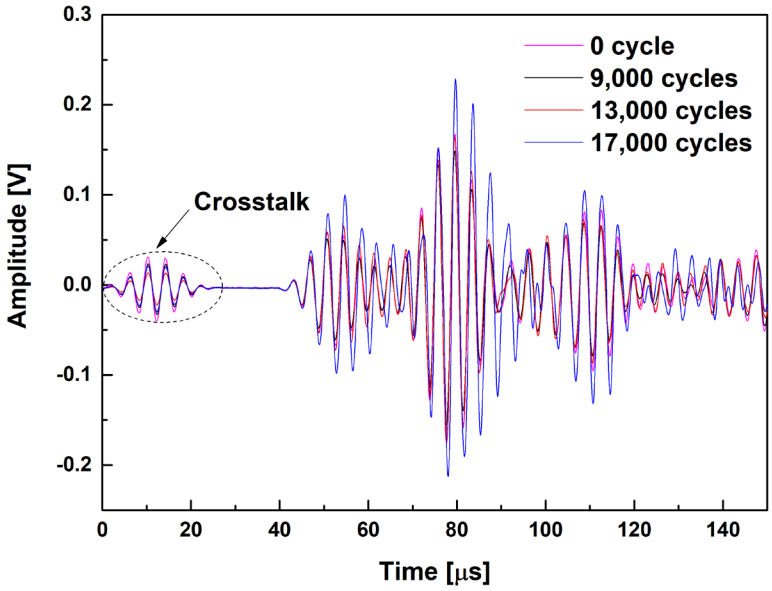

378
379 (a)

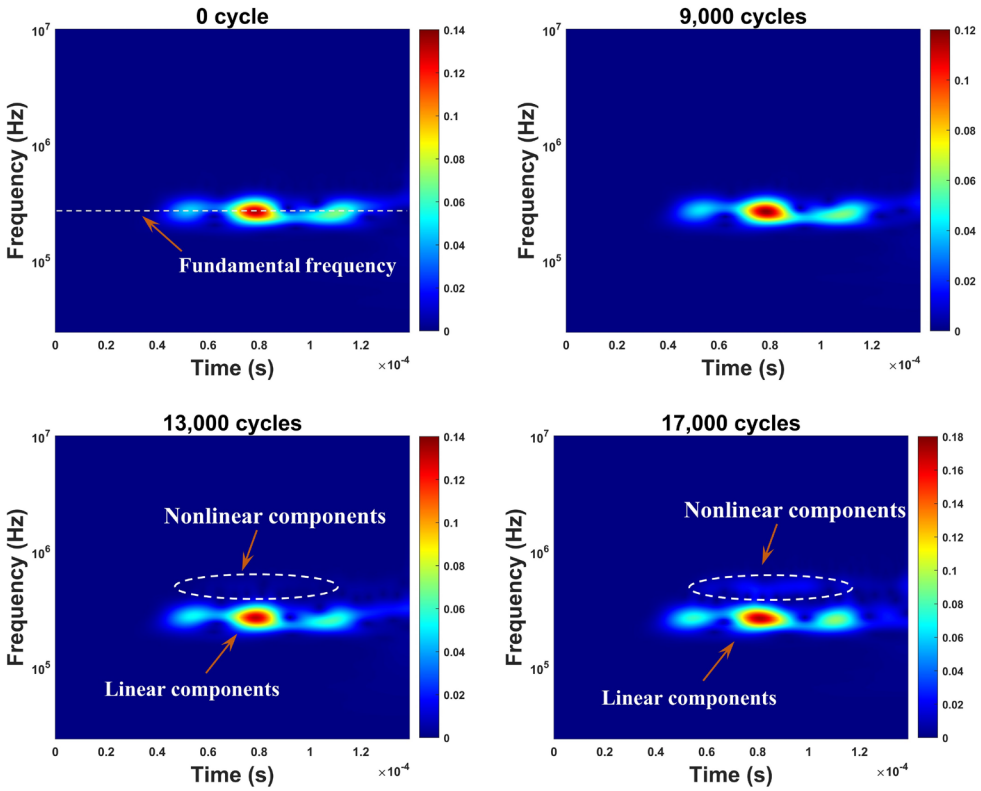

(b)

Fig. 8. (a) Typical UGW signals captured from Specimen 1 at different fatigue cycles; and (b) the corresponding spectra of the selected GUW signals obtained via the CWT.

The RGB images of the spectra of the experimental UGW signals acquired from Specimen 1 and Specimen 2, embracing both linear and nonlinear features of the captured UGWs, are collected to construct an image dataset for subsequent training and validation of the proposed DenseNet-based regression model. All the images are scaled to 224×224 before training and validation, to match the input unit of the DenseNet.

Due to the experimental data is insufficient to train a DL model, FEM simulation is conducted for the purpose of dataset expansion. 57 FE models are built to obtain synthetic UGW signals from waveguides with corner cracks of different severities (crack length and depth ranging from 1 to 3 mm) emanating from a fastener hole. In each simulation case, two sensing points with the same locations of the two sensors used in experiment are selected to acquire UGW signals. The pulse-

396 inversion technique adopted in the experiment is also utilized in the FEM simulation, leading to
397 a total of 228 artificial UGW signals obtained from the simulation.
398
399 Reliable and verified FEM simulation results are crucial for training the proposed model. A
400 representative simulated UGW signal captured from the waveguide containing a conner crack
401 with the length of 1.2 mm and depth of 1.5 mm is illustrated in **Fig. 9**, and further compared with
402 its experimental counterpart which is obtained from Specimen 2 when the corner crack measuring
403 1.201 mm long and 1.514 mm deep at 17,000 cycles. For better comparison, the simulated and
404 experimental UGW signals are normalized by their peak values, respectively. It can be observed
405 that the simulated signal is in good agreement with the experimental signal, especially in the first-
406 arrival wave packet as highlighted in the dashed region, which contains the majority of the crack-
407 related UGW information. It is therefore concluded that the FEM simulation is able to provide
408 reliable synthetic UGW signals to expand dataset for training the model.
409

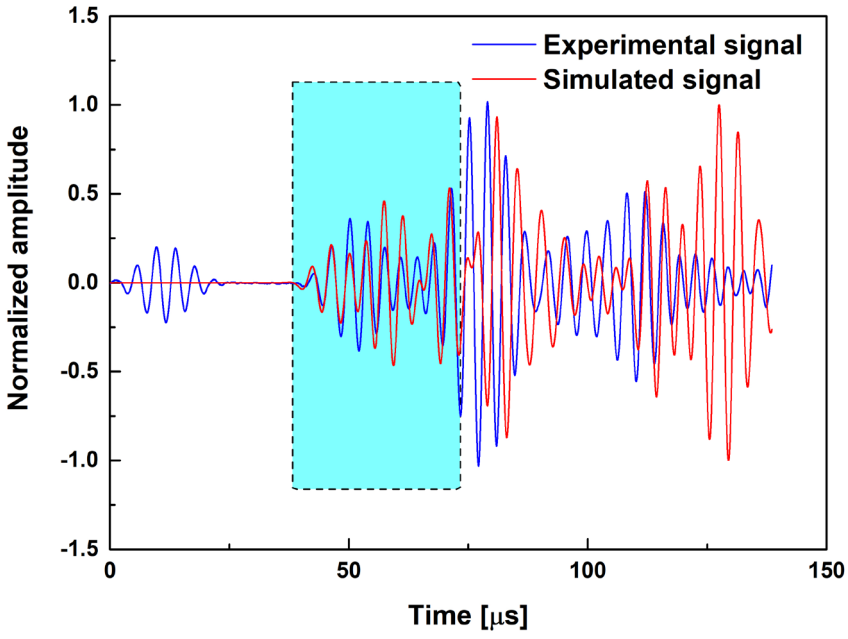

410

411 **Fig. 9.** The simulated UGW signals obtained from the waveguide containing a corner crack with the length of
412 1.2 mm and depth of 1.5 mm and the comparison with its experimental counterpart.
413

The CWT is subsequently recalled to convert the synthetic UGW signals obtained from FEM simulation into RGB images for dataset expansion for a better training performance. Like the images obtained from experimental signals, the spectral images of simulated signals are also re-sized to 224×224 to fulfill the requirement of DenseNet.

4.2 Dataset for Model Training and Validation

Based on the experiment and FEM simulation, a total of 400 data samples, including 178 experimental data and 228 simulation data, are collected and split to build the training and validation datasets, for the training and validation of the proposed DenseNet-based model. As illustrated in **Fig. 10**, the training dataset (360 data) accounts for 90 % of the total acquired data, consisting of all simulation data and part of the experimental data (132 data). The remaining 10 % of the total data is utilized to construct the validation dataset comprising pure experimental data, to demonstrate the effectiveness of the trained model in predicting the length and depth of the corner crack using real-world UGW signals.

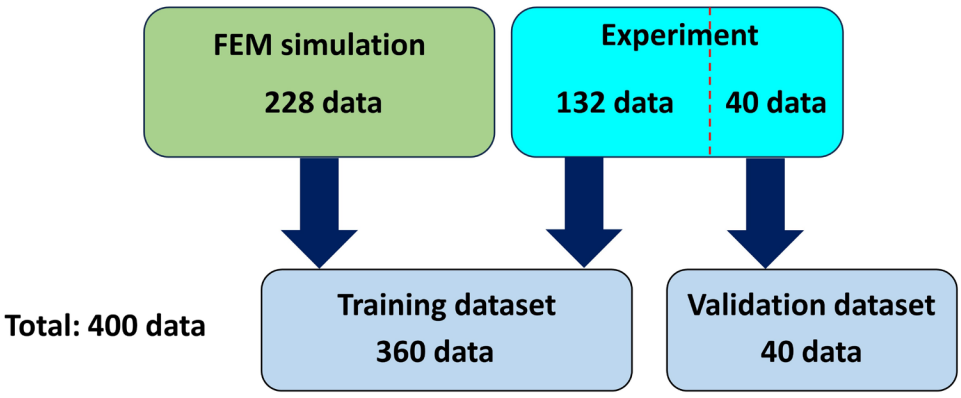

Fig. 10. Allocation of simulation and experimental data for model training and validation.

4.3 Training and Validation Results

With the training dataset containing both simulated and experimental data, the training of the proposed DenseNet-based regression model is implemented on a computer with 64 Gigabytes

RAM, an Intel(R) Core(TM) i9-11900K CPU @ 3.50 GHz and a NVIDIA GeForce RTX 3080 GPU. The batch size and the number of training epoch are set to be 18 and 100, respectively, resulting in a total of 2,000 iterations (the parameters of the model are updated in every single iteration) throughout the entire training process. Adam optimizer is utilized to optimize the training efficiency, considering its superb merits in terms of convergence speed, memory requirement and generalization to new data. The learning rate is initially set to be 0.001 and then dynamically adjusted as the training progresses according to a pre-defined schedule, to prevent the chaotical bounce around the local minimum value.

The mean squared error (MSE) is chosen as the loss function as it is appropriate to update the model parameters in regression tasks, which is defined as

$$MSE = \frac{1}{N}\sum_{i=1}^{N}(x_i - \hat{x}_i)^2, \tag{2}$$

where N is the batch size, x_i and $\hat{x}_i$ represent the true and predicted values, respectively. **Fig. 11** displays the variation of the training loss within the 100 epochs of the training process, from which it can be observed that the loss drastically drops in the first few epochs, then gradually decreases and finally stabilizes at around 0.006. The minimum value of the model loss during the whole training process is 0.00562 at the 92nd epoch. The rapid convergence of the loss value verifies the effectiveness of the training of the proposed model using the combination of simulated and experimental data.

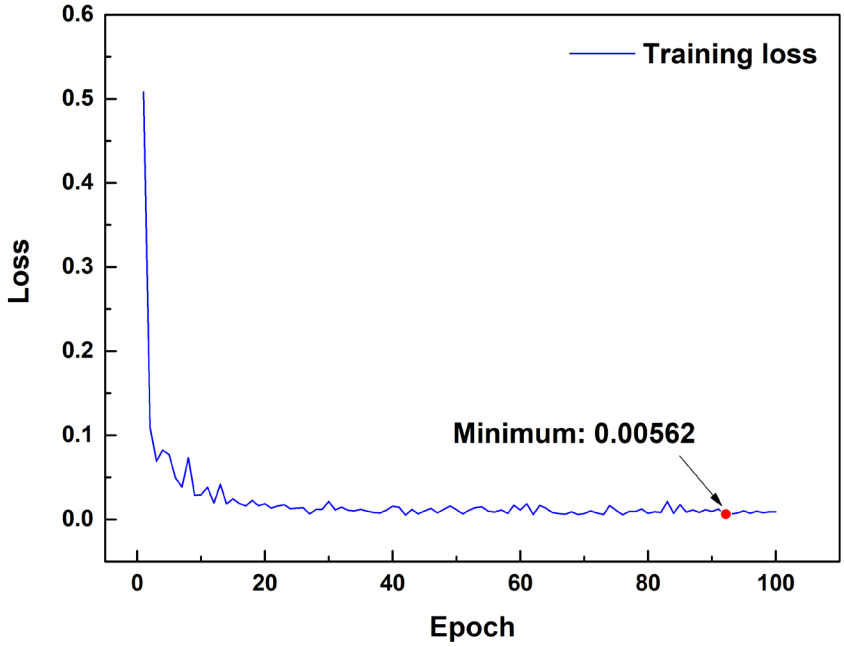

Fig. 11. The loss of the proposed regression model during the training process.

The validity of the proposed DenseNet-based regression model in evaluating the severity of 3D fatigue cracks is testified by applying the trained model to predict the length and depth of the corner crack in the two specimens using the validation dataset. **Fig. 12** illustrates the predicted results as well as the comparison with true values measured in the experiment. Good agreement between the predicted and measured results throughout the whole fatigue crack growth testing has demonstrated that the proposed regression model is capable of evaluating 3D fatigue cracks not only in their embryonic stage, also in the stable growth stage, in a continuous and quantitative manner. The relative errors of the crack length and depth predicted by the trained model are summarized in **Table 1**, from which it can be found that the maximum relative error in the two specimens is 5.97 %, showing the high accuracy of the model prediction.

Table 1. Summary of the relative errors of model prediction.

	Relative error of crack length (%)		Relative error of crack depth (%)	
	Maximum	Mean	Maximum	Mean
Specimen 1	5.69	2.30	5.83	2.69
Specimen 2	3.95	1.14	5.97	1.70

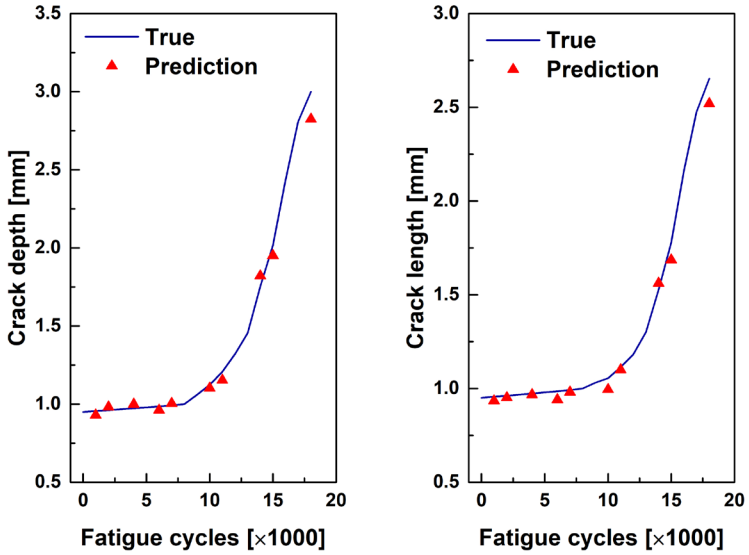

(a)

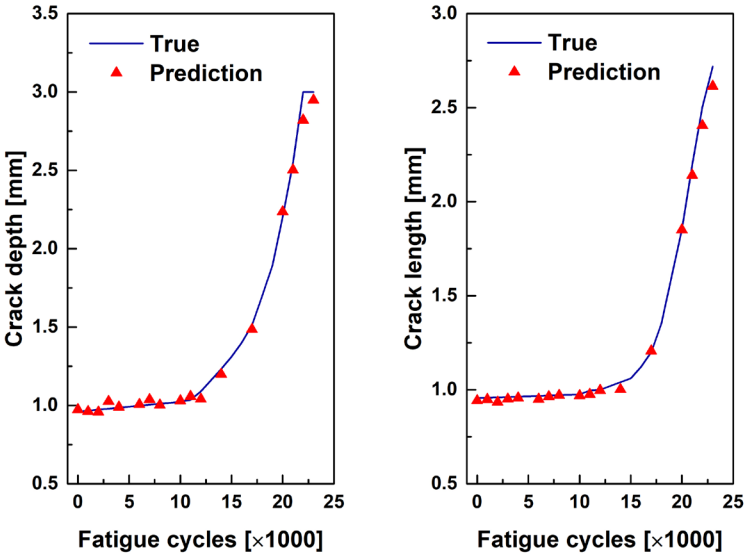

(b)

Fig. 12. Predicted length and depth of the corner crack in (a) Specimen 1 and (b) Specimen 2 using the trained DenseNet-based regression model, as well as the comparison with experimental results.

4.4 Comparison Study

A comparison study is conducted to highlight the superb merit of the proposed DenseNet-based regression model over previously reported nonlinear UGW-based model in the assessment of 3D fatigue cracks, spanning from crack initiation, through stable growth, to macroscopic crack formation. Based on the elastodynamic analysis, the nonlinear interaction between a fatigue crack

and probing UGW was scrutinized and a crack-surface-area-dependent nonlinear damage index was proposed for characterizing the severity of fatigue cracks [16]. To take a step further, a two-step, 3D fatigue crack assessment model capable of evaluating the crack length and depth was developed by combining the nonlinear damage index and the correlation between crack length and depth arising from a fatigue crack growth model [24]. In this section, the nonlinear UGW-based model is applied to evaluate the length and depth of the corner crack in Specimen 1 and Specimen 2 using the experimentally captured UGW signals. **Fig. 13.** compares the predicted results of the proposed DenseNet-based regression and the nonlinear UGW-based model.

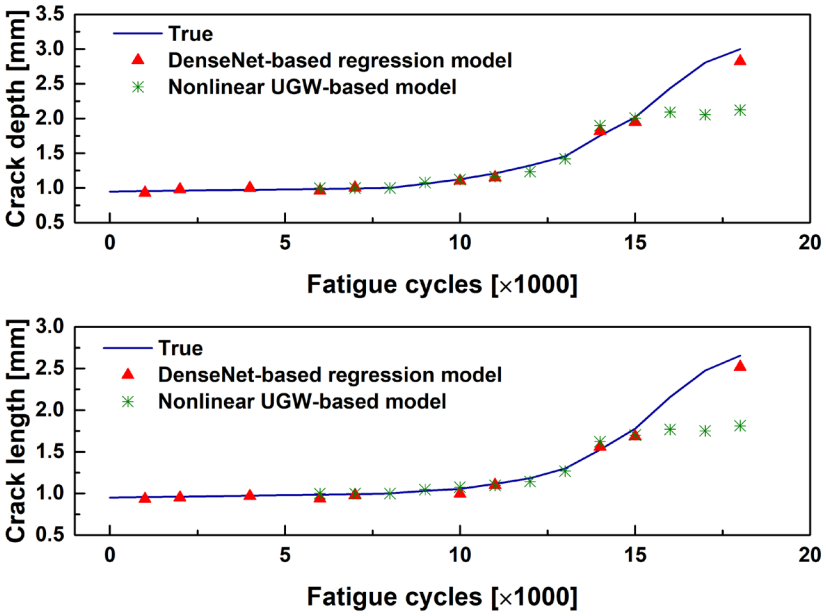

(a)

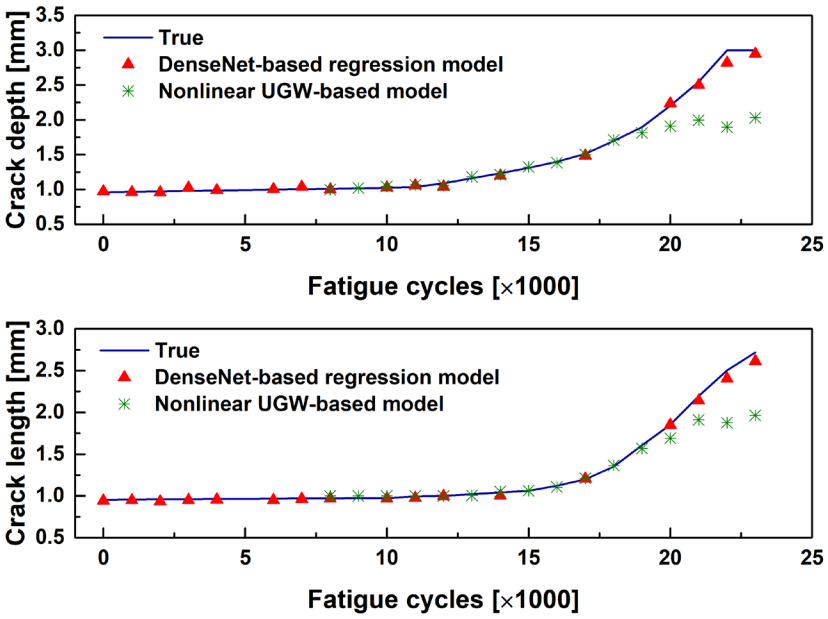

(b)

Fig. 13. Length and depth of the corner crack in (a) Specimen 1 and (b) Specimen 2 predicted by the proposed DenseNet-based regression model and the nonlinear UGW-based model [24], as well as the comparison with experimental results.

It can be observed from **Fig. 13** that both models can predict the crack length and depth with high accuracy during the crack initiation and the early stage of crack growth when the crack size is less than 2 mm, for example, the first 15,000 fatigue cycles of Specimen 1 and the first 19,000 fatigue cycles of Specimen 2. However, the nonlinear UGW-based model fails to assess the crack severity when a macroscopic crack is formed (*i.e.*, crack grows beyond 2 mm in this study). In this stage, dimensions of the crack are relatively large, and the large crack opening displacement imposes restrictions on the nonlinear modulation of the crack on the probing UGW, leading to the inapplicability of the nonlinear damage index. On the contrary, by learning both linear and nonlinear features of the captured UGW signals, the proposed DenseNet-based regression model can still evaluate the severity of the crack even when the corner crack has already penetrated the whole thickness of the specimen, demonstrating its usability throughout the initiation and growth stages of 3D fatigue cracks.

5. Concluding Remarks

A DL-based regression model making use of the DenseNet framework is developed in this study, targeting quantitative evaluation of 3D, non-penetrating fatigue cracks from their embryonic initiation, through progressive growth to formation of macroscopic cracks. CWT is adopted to convert the UGW signals into RGB images representing their time-frequency domain spectra, which includes both linear and nonlinear features of UGW signals. The spectra images are subsequently used as the input of the DenseNet to extract implicit features. The last fully connected layer of DenseNet is modified as a regression layer to predict the length and depth of the 3D fatigue crack. To validate the effectiveness of the proposed DenseNet-based regression model, fatigue crack growth and ultrasonic testing is performed to acquire UGW signals during the initiation and growth stages of a corner crack emanating from a fastener hole. FE simulation is further conducted for dataset expansion. The collected experimental and simulated data are split into training and validation datasets, for training and verifying the proposed model, respectively. A comparison study is undertaken and the results demonstrate that compared with previously reported nonlinear UGW-based model, the proposed DenseNet-based regression model can evaluate the length and depth of 3D fatigue cracks with high accuracy not only in the crack initiation stage, but also in the stable growth stage, showing its versatility in early awareness and long-term assessment of fatigue cracks.

Acknowledgements

The support from the Innovation and Technology Commission (ITC) of the Hong Kong SAR Government via AIR@InnoHK is gratefully acknowledged. The work was also supported by CRD projects of Hong Kong Productivity Council (Nos. 10013288 and 10014870). Z Su acknowledges the support from the Hong Kong Research Grants Council via General Research Funds (Nos. 15200922, 15202820 and 15204419).

References

[1] S. Li, Q. Liu, S.-S. Rui, X. Li, M. Hu, K. Li, Q. Sun, Z. Cai, J. Pan, Fatigue crack initiation behaviors around defects induced by welding thermal cycle in superalloy IN617B, International Journal of Fatigue, 158 (2022) 106745.

[2] G. Zhao, M. Jiang, W. Li, Y. Luo, Q. Sui, L. Jia, Early fatigue damage evaluation based on nonlinear Lamb wave third-harmonic phase velocity matching, International Journal of Fatigue, 167 (2023) 107288.

[3] Y. Zhu, F. Li, W. Bao, Fatigue crack detection under the vibration condition based on ultrasonic guided waves, Structural Health Monitoring, 20 (2021) 931-941.

[4] S. Sampath, H. Sohn, Detection and localization of fatigue crack using nonlinear ultrasonic three-wave mixing technique, International Journal of Fatigue, 155 (2022) 106582.

[5] E.C. Rodgers, S. Mariani, P. Cawley, The use of circumferential guided waves to monitor axial cracks in pipes, Structural Health Monitoring, 22 (2023) 2609-2625.

[6] W. Zhu, Z. Xu, Y. Xiang, C. Liu, M. Deng, X. Qiu, D. Sun, F. Xuan, Nonlinear ultrasonic detection of partially closed cracks in metal plates using static component of lamb waves, NDT & E International, 124 (2021) 102538.

[7] M. Zhao, W. Zhou, Y. Huang, H. Li, Sparse Bayesian learning approach for propagation distance recognition and damage localization in plate-like structures using guided waves, Structural Health Monitoring, 20 (2021) 3-24.

[8] Y. Lu, L. Ye, Z. Su, C. Yang, Quantitative assessment of through-thickness crack size based on Lamb wave scattering in aluminium plates, NDT & E International, 41 (2008) 59-68.

[9] W. Leong, W.J. Staszewski, B. Lee, F. Scarpa, Structural health monitoring using scanning laser vibrometry: III. Lamb waves for fatigue crack detection, Smart Materials and Structures, 14 (2005) 1387.

[10] H. Cho, C.J. Lissenden, Structural health monitoring of fatigue crack growth in plate structures with ultrasonic guided waves, Structural Health Monitoring, 11 (2012) 393-404.

[11] J. He, X. Guan, T. Peng, Y. Liu, A. Saxena, J. Celaya, K. Goebel, A multi-feature integration method for fatigue crack detection and crack length estimation in riveted lap joints using Lamb waves, Smart Materials and Structures, 22 (2013) 105007.

[12] W. Ostachowicz, P. Kudela, P. Malinowski, T. Wandowski, Damage localisation in plate-like structures based on PZT sensors, Mechanical Systems and Signal Processing, 23 (2009) 1805-1829.

[13] B. Masserey, P. Fromme, In-situ monitoring of fatigue crack growth using high frequency guided waves, NDT & E International, 71 (2015) 1-7.

[14] C. Yeung, C.T. Ng, Time-domain spectral finite element method for analysis of torsional guided waves scattering and mode conversion by cracks in pipes, Mechanical Systems and Signal Processing, 128 (2019) 305-317.

[15] F. Wen, S. Shan, L. Cheng, Third harmonic shear horizontal waves for material degradation monitoring, Structural Health Monitoring, 20 (2021) 475-483.

[16] L. Xu, Y. Su, K. Wang, X. Yang, S. Yuan, Z. Su, An elastodynamic reciprocity theorem-based closed-form solution to second harmonic generation of lamb waves by a fatigue crack: Theory & experimental validation, Journal of Sound and Vibration, 509 (2021) 116226.

[17] T. Ye, S. Biwa, N. Mori, Second-harmonic generation of the lowest-order antisymmetric Lamb wave at a closed parallel crack, The Journal of the Acoustical Society of America, 148 (2020) 2073-2085.

[18] I. Solodov, J. Wackerl, K. Pfleiderer, G. Busse, Nonlinear self-modulation and subharmonic acoustic spectroscopyfor damage detection and location, Applied Physics Letters, 84 (2004) 5386-5388.

[19] K.-A. Van Den Abeele, P.A. Johnson, A. Sutin, Nonlinear elastic wave spectroscopy (NEWS) techniques to discern material damage, part I: nonlinear wave modulation spectroscopy (NWMS), Journal of Research in Nondestructive Evaluation, 12 (2000) 17-30.

[20] C. Yeung, C.T. Ng, Nonlinear guided wave mixing in pipes for detection of material nonlinearity, Journal of Sound and Vibration, 485 (2020) 115541.
[21] H. Zhu, C.T. Ng, A. Kotousov, Frequency selection and time shifting for maximizing the performance of low-frequency guided wave mixing, NDT & E International, 133 (2023) 102735.
[22] W. Li, Y. Xu, N. Hu, M. Deng, Impact damage detection in composites using a guided wave mixing technique, Measurement Science and Technology, 31 (2019) 014001.
[23] H. Xu, L. Liu, J. Xu, Y. Xiang, F.-Z. Xuan, Deep learning enables nonlinear Lamb waves for precise location of fatigue crack, Structural Health Monitoring, (2023) 14759217231167076.
[24] L. Xu, K. Wang, X. Yang, Y. Su, J. Yang, Y. Liao, P. Zhou, Z. Su, Model-driven fatigue crack characterization and growth prediction: A two-step, 3-D fatigue damage modeling framework for structural health monitoring, International Journal of Mechanical Sciences, 195 (2021) 106226.
[25] J. Wang, Y. Shen, D. Rao, W. Xu, An instantaneous-baseline multi-indicial nonlinear ultrasonic resonance spectral correlation technique for fatigue crack detection and quantification, Nonlinear Dynamics, 103 (2021) 677-698.
[26] Y. Kim, H.J. Lim, H. Sohn, Nonlinear ultrasonic modulation based failure warning for aluminum plates subject to fatigue loading, International Journal of Fatigue, 114 (2018) 130-137.
[27] H. Alnuaimi, U. Amjad, P. Russo, V. Lopresto, T. Kundu, Monitoring damage in composite plates from crack initiation to macro-crack propagation combining linear and nonlinear ultrasonic techniques, Structural Health Monitoring, 20 (2021) 139-150.
[28] J. Deng, Y. Lu, V.C.-S. Lee, Imaging-based crack detection on concrete surfaces using You Only Look Once network, Structural Health Monitoring, 20 (2021) 484-499.
[29] X. Long, M. Yu, W. Liao, C. Jiang, A deep learning-based fatigue crack growth rate measurement method using mobile phones, International Journal of Fatigue, 167 (2023) 107327.
[30] S. Sampath, J. Jang, H. Sohn, Ultrasonic Lamb wave mixing based fatigue crack detection using a deep learning model and higher-order spectral analysis, International Journal of Fatigue, 163 (2022) 107028.
[31] S. Guo, H. Feng, W. Feng, G. Lv, D. Chen, Y. Liu, X. Wu, Automatic quantification of subsurface defects by analyzing laser ultrasonic signals using convolutional neural networks and wavelet transform, IEEE Transactions on Ultrasonics, Ferroelectrics, and Frequency Control, 68 (2021) 3216-3225.
[32] L. Zhu, Z. Wu, X. Hu, Y. Song, Investigation of small fatigue crack initiation and growth behaviour of nickel base superalloy GH4169, Fatigue & Fracture of Engineering Materials & Structures, 39 (2016) 1150-1160.
[33] J. Zhang, J. Zhu, W. Guo, W. Guo, A machine learning-based approach to predict the fatigue life of three-dimensional cracked specimens, International Journal of Fatigue, 159 (2022) 106808.
[34] J. Zhu, L. Xu, W. Guo, The influence of bending loading on surface fatigue crack growth life, International Journal of Fatigue, 167 (2023) 107285.
[35] R. Hao, P. Lehto, W. Lin, Critical distance-based fatigue life evaluation of blunt notch details in steel bridges, Journal of Constructional Steel Research, 201 (2023) 107738.
[36] G. Huang, Z. Liu, L. Van Der Maaten, K.Q. Weinberger, Densely connected convolutional networks, in: Proceedings of the IEEE conference on computer vision and pattern recognition, 2017, pp. 4700-4708.
[37] Y. Ohara, K. Kawashima, R. Yamada, H. Horio, Evaluation of amorphous diffusion bonding by nonlinear ultrasonic method, in: AIP Conference Proceedings, American Institute of Physics, 2004, pp. 944-951.
[38] K. Wang, Y. Li, Z. Su, R. Guan, Y. Lu, S. Yuan, Nonlinear aspects of "breathing" crack-disturbed plate waves: 3-D analytical modeling with experimental validation, International Journal of Mechanical Sciences, 159 (2019) 140-150.
[39] W. Cao, K. Wang, P. Zhou, X. Yang, L. Xu, M. Liu, P. Fromme, B. Pang, R. Chi, Z. Su, Nonlinear ultrasonic evaluation of disorderedly clustered pitting damage using an in situ sensor network, Structural Health Monitoring, 19 (2020) 1989-2006.

[40] H. Chen, Z. Feng, Y. Du, Q. Chen, H. Miao, Spectral finite element method for efficient simulation of nonlinear interactions between Lamb waves and breathing cracks within the bi-potential framework, International Journal of Mechanical Sciences, 215 (2022) 106954.
[41] N.P. Yelve, M. Mitra, P.M. Mujumdar, Spectral damage index for estimation of breathing crack depth in an aluminum plate using nonlinear Lamb wave, Structural Control and Health Monitoring, 21 (2014) 833-846.
[42] Y. Shen, J. Wang, W. Xu, Nonlinear features of guided wave scattering from rivet hole nucleated fatigue cracks considering the rough contact surface condition, Smart Materials and Structures, 27 (2018) 105044.